Phys Chem Minerals (1991) 18:171–179

PHYSICS AND CHEMISTRY OF MINERALS

Back Transformation and Oxidation of $(Mg, Fe)_2SiO_4$ Spinels at High Temperatures

L.C. Ming[1], **Y.H. Kim**[2], **M.H. Manghnani**[1], **S. Usha-Devi**[3], **E. Ito**[4], **and H.-S. Xie**[5]

[1] Mineral Physics Group, Department of Geology and Geophysics, University of Hawaii, Honolulu HI 96822, USA
[2] Department of Geology, Gyeongsang National University, Jinju 660-701, Korea
[3] National Aeronautical Laboratory, Bangalore 560017, India
[4] Institute of Study of the Earth's Interior, Okayama University, Misasa, Tottorri-ken 682-02, Japan
[5] Institute of Geochemistry, Academia Sinica, Guiyang, PR China

Received April 18, 1990 / Accepted March 4, 1991

Abstract. Based on the in situ and temperature-quench X-ray measurements, the back transformation in the $(Mg, Fe)_2SiO_4$-spinels has been characterized in terms of the transformation temperature (T_r), mechanism and kinetics of the transformation, and of the end product(s), with specific emphasis on the effect of oxygen on this transformation. The in situ measurements were conducted to 900° C in vacuum (10^{-4} to 10^{-5} torr) and to 600° C in air using *synchrotron radiation* (SR) at Stanford Synchrotron Radiation Laboratory (SSRL). In the quench-type measurements, samples were heated in air to 1100° C, quenched and examined at ambient conditions using the conventional X-ray diffraction facilities. Important results are (1) in vacuum, all the spinels convert back into the olivine phase, with their T_r decreasing with increasing iron content; (2) the spinel → olivine back transformation is a nucleation and growth type of transformation and can be described quantitatively using the Avrami equation; (3) in air, the $(Mg, Fe)_2SiO_4$-spinels with 0.2 mole fraction Fe or more are all oxidized, and the composition and phase of the end products depend upon the temperature and the starting composition; and (4) the oxidation of the iron-rich $(Mg, Fe)_2SiO_4$-spinels in air occurs at ~350–400° C, which is significantly lower than its T_r (~300° C) in vacuum.

Introduction

In the system $(Mg, Fe)_2SiO_4$, the olivine → spinel transition is observed at 6 GPa and 1000° C for pure Fe_2SiO_4 and at 17–21 GPa and 1000° C for pure Mg_2SiO_4 (e.g., Akimoto and Fujisawa 1968; Ringwood and Major 1970; Suito 1972, 1977; Kawada 1977; Katsura and Ito 1989). It has also been demonstrated that this transition can proceed either via the nucleation and growth mechanism under low shear stress conditions (Sung and Burns 1976a, b) or via the martensitic mechanism in a high shear stress environment (e.g., Poirier 1982; Furnish and Bassett 1983; Lacam et al. 1980; Boland and Liu 1983). Since the $(Mg, Fe)_2SiO_4$-olivine is the most abundant mineral phase in the Earth's upper mantle, its transformation into the spinel phase under high pressure and high temperature conditions has many important geophysical implications. Such a transformation has provided a plausible explanation for the seismic discontinuity at a depth of 400 km (e.g., Akimoto et al. 1976; Ringwood 1975; Jeanloz and Thompson 1983; Bina and Wood 1987; Weidner and Ito 1987), a potential triggering mechanism for deep-seated earthquakes (e.g., Sung and Burns 1976a, b), and a driving force for the downgoing slab of the oceanic crust (e.g., Ringwood 1975). According to the pyrolite model (e.g., Ringwood 1975; Weidner 1985), the $(Mg, Fe)_2SiO_4$-spinel is regarded to be the most abundant mineral phase in the transition zone (i.e., at depths between 400 and 670 km).

Recently Knittle and Jeanloz (1987) have carried out a back transformation (i.e., perovskite → enstatite) study on $(Mg, Fe)SiO_3$-perovskite at 1 bar and obtained valuable information pertaining to the mechanism and kinetics of the back transformation, shedding new light on mantle dynamics. In this context we were motivated to carry out such a study on $(Mg, Fe)_2SiO_4$-spinels, presumably one of the most abundant minerals in the Earth's mantle at depths between 400 and 670 km. As several important physical properties such as thermal expansion, heat capacity, and the heat of formation (enthalpy) of $(Mg, Fe)_2SiO_4$-spinels have been measured at high temperatures and at 1 bar pressure, it would be extremely valuable to understand the possible effect of the oxygen on the back transformation of this phase at high temperatures.

The main purpose of this paper is to demonstrate that the presence of oxygen in the experimental conditions (i.e., runs in air vs. those made in vacuum), indeed, has remarkable effect on the back transformation in $(Mg, Fe)_2SiO_4$ spinels.

Experimental Methods

Samples

Polycrystalline spinel samples of four compositions (Mg_2SiO_4, $(Mg_{0.8}, Fe_{0.2})_2SiO_4$, $(Mg_{0.6}, Fe_{0.4})_2SiO_4$, and $(Mg_{0.4}, Fe_{0.6})SiO_4$) were synthesized at pressures between 10 and 22 GPa and at 1200° C at the Institute for Study of the Earth's Interior, Okayama University. The fifth spinel sample (Fe_2SiO_4) was synthesized from a stoichiometric mixture of Fe_2O_3 and SiO_2 at 6 GPa and 1200° C at the Geochemistry Institute, Academia Sinica, Kuenyoung, China. All the samples were identified using X-ray diffraction technique as the pure spinel phase.

Experimental Procedure

In addition to the quench-type experiments performed by Knittle and Jeanloz (1987), we have carried out the in situ X-ray diffraction studies in a *diamond-anvil cell* (DAC) using *synchrotron radiation* (SR). The advantages of in situ X-ray diffraction measurements with SR are (1) the back transformation at each temperature can be observed in real time; (2) at each temperature, only one sample run is needed for completion of a time-dependent experiment, thus minimizing the consumption of the high-pressure phase; (3) X-ray diffraction data can be obtained in a much shorter time period (e.g., 1–3 min) and is thus able to provide many more data points at each temperature than the quenched experiment with a conventional X-ray source; and (4) additional thermal expansion data for the (Mg, Fe)$_2$SiO$_4$-spinel samples could also be obtained preceding the back transformation during the run. The experimental procedures involved in the two types of experiments are given below.

In situ high temperature experiments. In this study, the spinel sample was heated either in air or in vacuum (10^{-4} to 10^{-5} torr) in an improved DAC equipped with a micro-resistive heater (Ming et. al. 1987) and X-rayed under the in situ high temperature conditions using the energy dispersive X-ray diffraction technique. All the in situ high-temperature runs were carried out at Stanford Synchroton Radiation Laboratory (SSRL). The experimental setup at SSRL and temperature calibration procedures in the DAC have been described previously (Ming et. al. 1983, 1987). The X-ray diffraction data were collected by an intrinsic Ge detector with $2\theta \sim 14°$. With the storage ring operating at 3 GeV and 30–60 mA, each spectrum was collected for 3–10 min in the live-time mode. Runs conducted in vacuum were carried out to 900° C and those made in air were limited below 650° C in order to prevent the oxidation of tungsten carbide and the graphitization of diamond anvils.

Quench-type experiments. In these experiments, the sample was loaded in the hole (0.3 mm in diameter) of the Inconel gasket (0.125 mm thick) and heated in air to a desired temperature for an hour in a laboratory furnace. The heated sample was then quenched in air and X-rayed at ambient conditions in a modified Debye-Scherrer camera using a fine-focused radiation (either the Ni-filtered Cu-K_α or the Zr-filtered Mo-K_α). With the "in-house" X-ray generator operating at 40 kV and 15 mA (for a Philips generator with a Cu target) or at 50 kV and 26 mA (for a Enraf-Nonius generator with a Mo target), the exposure time for obtaining a high quality X-ray diffraction pattern for each sample was 70–100 h.

Results and Discussions

Studies in Vacuum

(Mg, Fe)$_2$SiO$_4$-spinel, a high pressure phase of (Mg, Fe)$_2$SiO$_4$-olivine, is stable at pressures above 6.0 GPa. It is anticipated that by heating the spinel phase at pressures below 6.0 GPa, it should convert back to stable low-pressure phase with the olivine structure. In order to avoid any possible effect of oxygen on the back transformation of (Mg, Fe)$_2$SiO$_4$-spinels, we first performed the experiments in vacuum (10^{-4} to 10^{-5} torr) to ~900° C. In situ X-ray diffraction data revealed that all the (Mg, Fe)$_2$SiO$_4$ spinels indeed convert back to olivines, and that T_r decreases with decreasing Mg content such that $T_r \sim 800$, 735, and 620° C for Mg_2SiO_4, $(Mg_{0.8}, Fe_{0.2})_2SiO_4$, $(Mg_{0.4}, Fe_{0.6})_2SiO_4$ spinels, respectively. It has also been observed that at temperature between 760 and 900° C, all the above spinels convert back completely into their corresponding olivine phase in 2 h. X-ray spectra elucidating the time-dependence of the spinel → olivine transformation at 760° C are shown in Fig. 1.

For an isochemical high-pressure phase transformation, the relative amounts of the high-pressure and low-pressure phases can be determined from X-ray intensity data (e.g., Zeto and Roy 1969; Brar and Schloessin 1981; Hamaya and Akimoto 1982; Manghnani et al. 1987). In this study, the amount of olivine phase transformed from

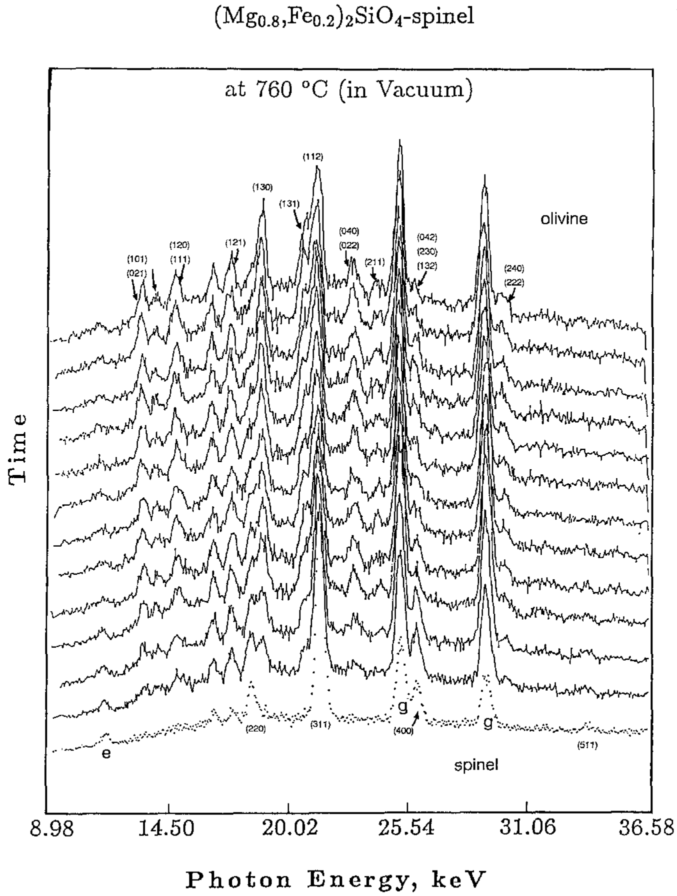

Fig. 1. Selected energy spectra of $(Mg_{0.8}, Fe_{0.2})_2SiO_4$-sp at 760° C (in vacuum) as a function of time. It shows that the spinel phase (the lowest spectrum) gradually converts back into the olivine phase (the uppermost spectrum). The total time between the lowest and the uppermost spectrum is ~2 h. The peak labelled with e indicates the escape peak and those with g, the gasket peak

the spinel phase as a function of time is calculated on the basis of the following relationship:

$$X_{ol} = I_{ol(112))}/[I_{ol(112)} + I_{sp(311)}] \tag{1}$$

where X_{ol} is the fraction of the olivine phase transformed, and $I_{ol(112)}$ and $I_{sp(311)}$ are the most intense diffraction peaks for olivine and spinel, respectively. Since the ol(112) diffraction peak overlaps with that of sp(311), the sum of their intensities can be directly obtained from the sp(311) peak intensity. The value of $I_{ol(112)}$ in Eq. (1) can be estimated from the ol(130) peak intensity, which is ~62%, 71% and 85% of $I_{ol(112)}$, for Mg_2SiO_4, $(Mg_{0.8}, Fe_{0.2})_2SiO_4$, and $(Mg_{0.4}, Fe_{0.6})_2SiO_4$, respectively (Jahanbagloo 1969). Equation (1) can therefore be written as

$$X_{ol} = C \times I_{ol(130)}/[I_{ol(112)} + I_{sp(311)}] \tag{2}$$

where the constant C is a conversion factor between $I_{ol(130)}$ and $I_{ol(112)}$, and calculated to be 1.61, 1.41 and 1.18 for Mg_2SiO_4, $(Mg_{0.8}, Fe_{0.2})_2SiO_4$, and $(Mg_{0.4}, Fe_{0.6})_2SiO_4$ respectively.

Table 1. The fraction of the olivine phase (X) converted from the spinel phase as a function of time

Run #	Time (s)	X
(a) Mg_2SiO_4 at 900° C		
1356	720	0.15
1358	1080	0.24
1360	1440	0.29
1362	1800	0.47
1364	2160	0.46
1366	2520	0.61
1368	2880	0.74
1370	3240	0.84
1372	3600	0.87
1373	3960	0.88
1374	4320	0.89
1378	4680	0.999
(b) $(Mg_{0.8}, Fe_{0.2})_2SiO_4$ at 760° C		
1267	960	0.32
1268	1260	0.42
1269	1560	0.45
1270	1860	0.60
1271	2160	0.55
1272	2460	0.65
1273	2760	0.68
1274	3060	0.77
1275	3360	0.77
1277	3660	0.90
1278	3960	0.83
1281	4260	0.97
1282	4560	0.97
1283	4860	0.98
1284	5160	0.999
(c) $(Mg_{0.4}, Fe_{0.6})_2SiO_4$ at 800° C		
1325	860	0.35
1327	1220	0.51
1329	1580	0.64
1331	1940	0.80
1333	2300	0.82

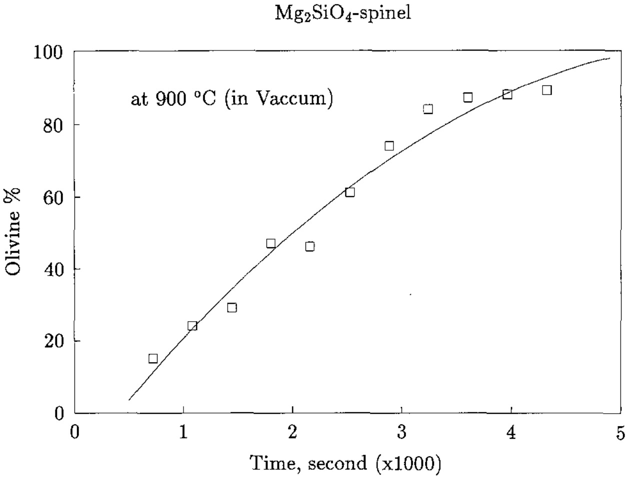

Fig. 2. The fraction of the olivine phase transformed from the spinel phase as a function of time for Mg_2SiO_4-sp at 900° C (in vacuum)

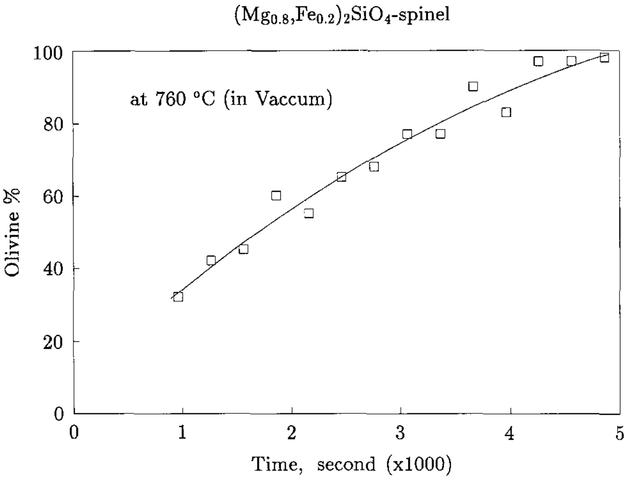

Fig. 3. The fraction of the olivine phase transformed from the spinel phase as a function of time for $(Mg_{0.8}, Fe_{0.2})_2SiO_4$-sp at 760° C (in vacuum)

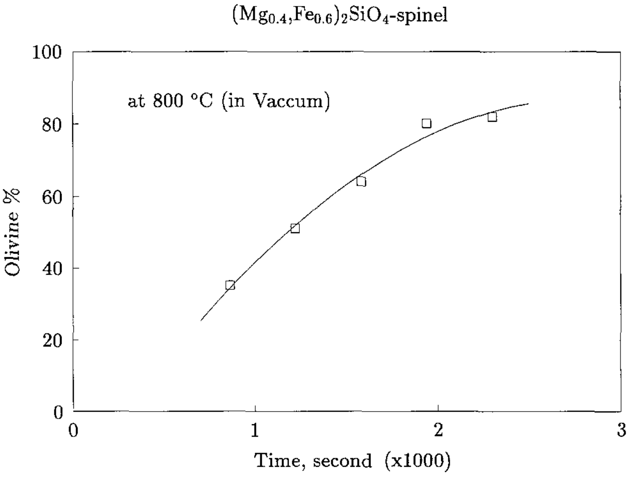

Fig. 4. The fraction of the olivine phase transformed from the spinel phase as a function of time for $(Mg_{0.4}, Fe_{0.6})_2SiO_4$-sp at 800° C (in vacuum)

The fractions of the olivine phase as a function of time for Mg_2SiO_4 spinel (at 900° C), $(Mg_{0.8}, Fe_{0.2})_2SiO_4$-spinel (at 760° C), and $(Mg_{0.4}, Fe_{0.6})_2SiO_4$-spinel (at 800° C) thus obtained using Eq. (2) are given in Table 1 and also plotted in Figs. 2, 3, and 4, respectively. These data clearly show that the spinel → olivine back transformation proceeds isothermally, that is, the olivine phase grows with time at the expense of the spinel phase. This is one of the unique characteristics of heterogeneous transformations involving nucleation and growth mechanism (e.g., Christian 1975). The kinetics rate for such a transformation has been described by the well-established Avrami equation expressed as:

$$X = 1 - \exp(-Kt^n) \qquad (3)$$

where X is the fraction of the new phase (i.e., the olivine phase in this study) growing with time t (in seconds) at constant pressure and temperature; K is a rate constant depending mainly on pressure, temperature, grain size and shear stress; and n is a mechanism-dependent constant. Equation (3) can be rewritten in a linear form as

$$\ln\ln[1/(1-X)] = \ln K + n \ln t \qquad (4)$$

where the values of K and n can be directly obtained from the intercept and the slope, respectively. Figures 5–7 are the plots of $\ln\ln[1/(1-X)]$ versus $\ln t$ for Mg_2SiO_4 spinel at 900° C, for $(Mg_{0.8}, Fe_{0.2})_2SiO_4$-spinel at 760° C, and for $(Mg_{0.4}, Fe_{0.6})_2SiO_4$-spinel at 800° C on the basis of the experimental data given in Table 1. Values of n and K derived from the regression analysis of these data are shown in Table 2.

According to the kinetics theory proposed by Cahn (1956), basically two stages are involved in a steady state transformation: (1) before all the nucleation sites on the grain surface are exhausted (generally in few minutes), the value of n is 4, and (2) after the saturation, the transformation proceeds only by growth, and the value of n quickly decreases to 1. Our results for n ranging from 1.48 to 1.56 obtained for spinel → olivine transformation in three spinels therefore indicate that during our measurements, the back transformation in spinel has already saturated all the nucleation sites on the surface of the spinel grains and has started to proceed from the grain boundaries and the surface into the interior of the spinel phases. Similar behavior was also found in the case of

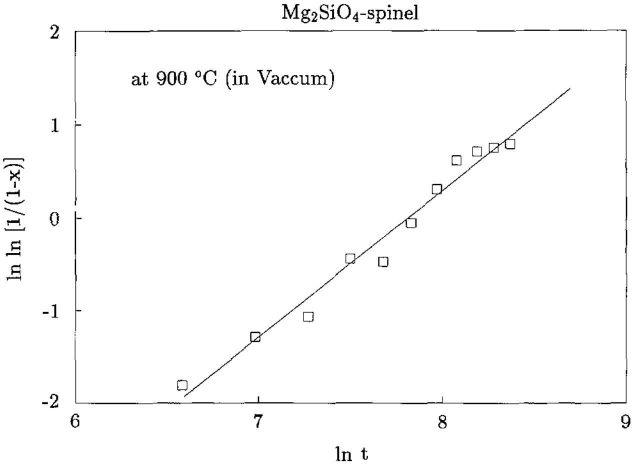

Fig. 5. The plot of $\ln\ln[1/(1-X)]$ versus $\ln t$ for Mg_2SiO_4-sp at 900° C (in vacuum). Linear regression of these data gives values of 4.8×10^{-6} and 1.56 for K and n, respectively

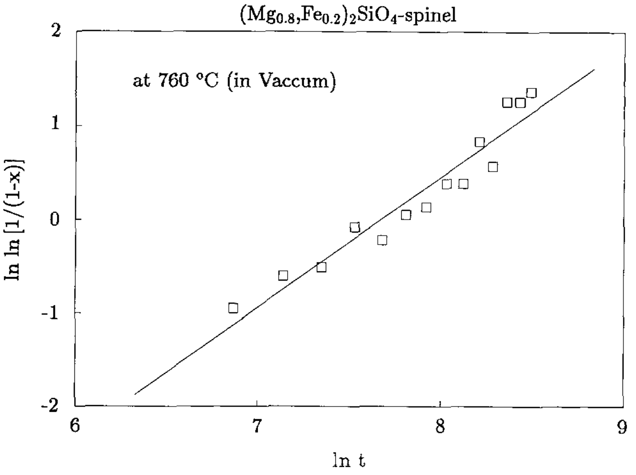

Fig. 6. The plot of $\ln\ln[1/(1-X)]$ versus $\ln t$ for $(Mg_{0.8}, Fe_{0.2})_2SiO_4$-sp at 760° C (in vacuum). Linear regression of these data gives values of 8.98×10^{-6} and 1.52 for K and n, respectively

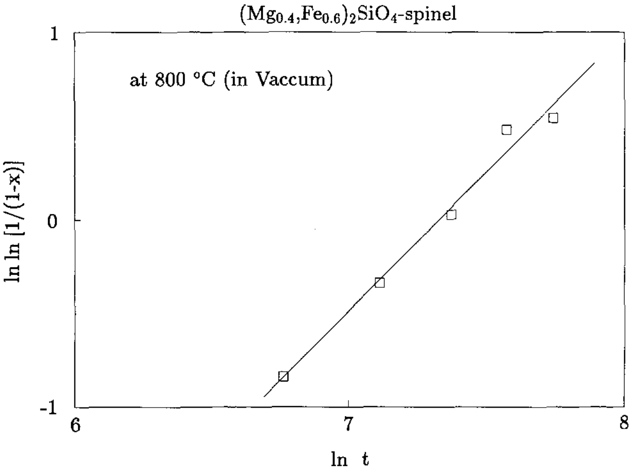

Fig. 7. The plot of $\ln\ln[1/(1-X)]$ versus $\ln t$ for $(Mg_{0.4}, Fe_{0.6})_2SiO_4$-sp at 800° C (in vacuum). Linear regression of these data gives values of 19.8×10^{-6} and 1.48 for K and n, respectively

Table 2. Values of n and K in Eq. (4) for various $(Mg, Fe)_2SiO_4$-spinels

Composition	Temperature	n	K, s^{-n}
Mg_2SiO_4	900	1.56	4.80×10^{-6}
$(Mg_{0.8}, Fe_{0.2})_2SiO_4$	760	1.52	8.98×10^{-6}
$(Mg_{0.4}, Fe_{0.6})_2SiO_4$	800	1.48	19.8×10^{-6}

$(Mg_{0.9}, Fe_{0.1})SiO_3$-perovskite transforming back to the enstatite phase (Knittle and Jeanloz 1987). It is also worth noting that at temperatures ranging from 760° C and 900° C, the kinetic rate constant (K) for the spinel → olivine back transformation in $(Fe, Mg)_2SiO_4$ (spinels) increases with increasing Fe content.

Studies in Air

One of the important questions concerning the back transformation of spinels is whether oxygen present in the system plays any role in the nature of this transition. In order to answer this question, in situ high-temperature X-ray diffraction measurements were carried out on the four spinel samples (except Fe_2SiO_4) in air at temperatures up to 594° C. Our preliminary in-situ X-ray diffraction data have shown that a new peak at ~18.95 keV ($d = \sim 270$ Å) appears in all the iron-rich spinels at temperatures around 350–400° C, which is about 300° C lower than those of T_r observed in vacuum. Assuming the back transformation to be spinel → olivine, Ming and Manghnani (1988) had initially interpreted this new peak to be (130) of olivine (the most intense peak in olivine) and thus suggested that oxygen present serves as a destabilizer for the iron-bearing spinels, facilitating the back transformation to occur at a much lower temperature than in vacuum.

However, detailed analysis of our in situ X-ray diffraction data at high temperatures does not support such interpretation. The d-spacings for all the new peaks observed for $(Mg_{0.4}Fe_{0.6})_2SiO_4$-spinel at 594° C have been calculated and compared (see Table 3) with those for $(Mg_{0.4}Fe_{0.6})_2SiO_4$-olivine calculated on the basis of the lattice parameters obtained at 600° C (Smyth 1975; Hazen 1977). As can be seen in Table 3, out of 7 non-overlapping peaks, only one peak at $d = 2.536$ Å matches with that of ol(131). All other six lines have d-spacings that deviate from those of olivine by 0.8 to 3%. These discrepancies are too large to be accounted for by the random errors (±0.1–0.2%) in the d-spacing measurements. The earlier tentative interpretation that spinel phase when heated at high temperatures in air transforms back into olivine phase is, therefore, not appropriate. The question remains as to the phases into which the spinel transforms. There are three possibilities:

Table 3. In-situ X-ray diffraction data for $(Mg_{0.4}, Fe_{0.6})_2SiO_4$-spinel heated using synchrotron radiation to 594° C in air

I/Io	d(obs.)	Spinel		Olivine	
		(hkl)	d(cal.)*	(hkl)	d(cal.)**
5	3.723 ?			(101)	3.753
20	2.904	(220)	2.907		
50	2.714 ?			(130)	2.794
35	2.536			(131)	2.536
100	2.480	(311)	2.480	(112)	2.481
5	2.241 ?			(140)	2.272
40	2.053	(400)	2.055		
10	1.868 ?			(150)	1.896
10	1.823 ?			(151)	1.809
10	1.711 ?			(222)	1.764
20	1.586	(511)	1.583		
40	1.454	(440)	1.453		

* Calculated on the basis of $a = 8.223(12)$ Å

** Calculated values using $a = 4.788$ Å, $b = 10.323$ Å and $c = 6.044$ Å which are estimated on the basis of lattice parameters obtained at 600° C for Mg_2SiO_4 (Hazen 1977) and for Fe_2SiO_4 (Smyth 1975)

(*a*) *Phase transformation*

$$(Mg, Fe)_2SiO_4(sp) \rightarrow (Mg, Fe)_2SiO_4(x)$$

where the unknown phase (x) would be one of the low-pressure or high-temperature phases such as the phenacite phase or the β-K_2SO_4 phase.

(*b*) *Chemical dissociation*

$$(Mg, Fe)_2SiO_4(sp) \rightarrow (Mg, Fe)SiO_3(en) + (Mg, Fe)O(mw)$$

where $(Mg, Fe)SiO_3(en)$ denotes orthoenstatite or clinoenstatite and (mw) denotes the magnesiowüstite phase.

(*c*) *Oxidation*

$$a(Mg, Fe)_2SiO_4(sp) + bO_2 \\ \rightarrow 2Fe_aO_b(x) + a\,MgSiO_3(en) + a\,MgO(pe)$$

or

$$(Mg, Fe)_2SiO_4(sp) + bO_2 \\ \rightarrow 2Fe_aO_b(x) + (Mg, Fe_{1-a})_2SiO_4(sp)$$

where $Fe_aO_b(x)$ could be Fe_2O_3 (hematite), Fe_3O_4 (magnetite), or FeO (wüstite) depending upon the oxygen availability, and (pe) represents the periclase phase.

In order to ensure the completion of the back transformation to either (a) or (b) or (c) described above and positive identification of the unknown phase(s), we pursued this study to much higher temperatures by employing a laboratory furnace. The latter was employed because the high-temperature DAC used in the in situ study in air was limited to temperatures up to 600° C (Ming and Manghnani 1988). The quench-type experiments were conducted for all the samples to 1100° C. The ambient X-ray diffraction data obtained for $(Mg_{0.4}Fe_{0.6})_2SiO_4$-spinel samples quenched from elevated temperatures are presented schematically in Fig. 8. These data, ranging from 500 to 1100° C, provide a fairly complete picture of the changes occurring in the spinel phase as a function of the quenched temperature. It is observed that the new peak ($d \sim 2.70$ Å), which first appears at 500° C, is the same peak that appeared at 430° C in our in situ runs made in air. Figure 8 also shows that the unknown phase grows gradually with temperature at the expense of the spinel phase and completely replaces the spinel phase at 1000° C. Comparing the X-ray diffraction data obtained at 1100° C with those of the olivine phase of the same composition, it is evident that the unknown phase is not the olivine phase. However, as can be seen in Fig. 9, the X-ray diffraction pattern at 1100° C can be correlated well with that of the

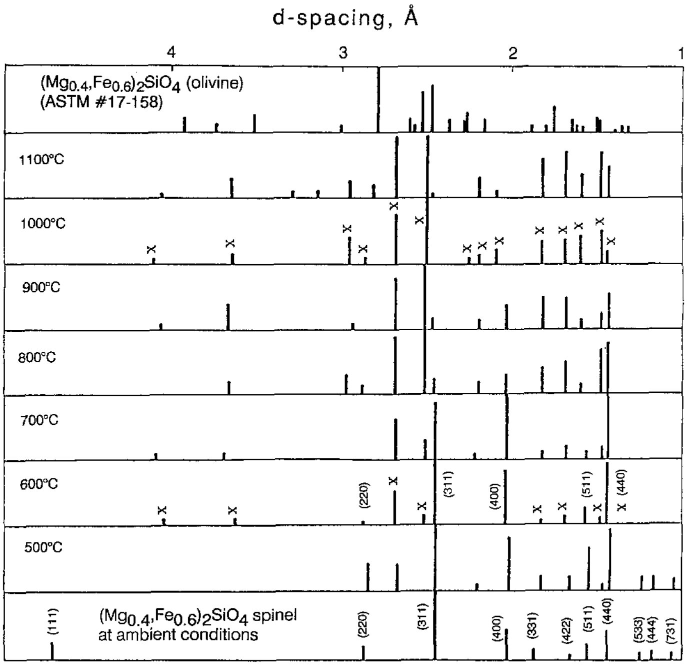

Fig. 8. Schematic X-ray diffraction diagrams showing the end product obtained by quenching the $(Mg_{0.4}, Fe_{0.6})_2SiO$-sp from various high temperatures. Those lines labelled with X represent the unknown phase(s) transformed from the spinel phase and do not match with those of the olivine phase as shown on the top

hematite and enstatite phases. On the basis of the assigned X-ray diffraction data listed (Table 4), the zero-pressure lattice parameters calculated for hematite are $a = 5.035$ Å and $c = 13.807$ Å, and for enstatite, $a = 18.412$ Å, $b = 8.781$ Å and $c = 5.218$ Å. These values are in fairly good agreement with the published data (i.e., hematite (ASTM # 13-534), $a = 5.034$ Å and $c = 13.796$ Å, and enstatite, (ASTM #19-770), $a = 18.22$ Å, $b = 8.829$ Å and $c = 5.192$ Å). Therefore, this is a oxidation reaction and can be expressed as follows

$$(2a+3b)(Mg_{0.4}, Fe_{0.6})_2SiO_4(sp) + 0.2aO_2$$
$$\rightarrow 1.2aFe_2O_3(hmt) + 1.2bFe_3O_4(mgt)$$
$$+ 0.4(2a+3b)\,MgSiO_3(en) + 0.6(2a+3b)\,SiO_2(x)$$

where a and b are the molar fractions of Fe_2O_3 and Fe_3O_4, respectively, and $a + b = 1$. $SiO_2(x)$ would be one of the low-pressure phases such as the α-quartz. Since no diffraction line for any SiO_2 polymorph was observed, it is most likely that any such SiO_2 phase would be present in the amorphous state.

Table 4. The X-ray diffraction data of $(Mg_{0.4}, Fe_{0.6})_2SiO_4$-spinel quenched from 1100° C

I/Io	d(obs.)	Phases identified			
		Fe_2O_3 (h)		$MgSiO_3$ (en)	
		(hkl)	d(cal.)*	(hkl)	d(cal.)**
5	4.807				
30	3.679	(012)	3.684		
10	3.319			(021)	3.305
10	3.168			(220)	3.168
25	2.981			(221)	2.980
20	2.844			(610)	2.872
				(511)	2.825
100	2.705	(104)	2.704		
				(421)	2.713
100	2.523	(110)	2.517	(131)	2.517
5	2.470			(430)	2.470
30	2.211	(113)	2.209		
10	2.119			(630)	2.118
60	1.842	(024)	1.843		
70	1.696	(116)	1.698		
35	1.613	(018)	1.605		
70	1.490	(214)	1.487		
50	1.455	(300)	1.453		

* d-spacings of the hematite phase, calculated on the basis of a hexagonal unit cell with lattice parameters of $a = 5.035$ Å, $c = 13.807$ Å

** d-spacing of the orthenstatite phase calculated on the basis of an orthorhombic unit cell with lattice parameters of $a = 18.412$ Å, $b = 8.781$ Å, $c = 5.218$ Å

It is interesting to note that at temperatures between 500 and 900° C, only hematite and spinel phases are present, indicating that the spinel phase preserved at such temperature conditions should be nonstoichiometric due to the iron loss during oxidation. The general oxidation reaction in these temperature range can be expressed as:

$$2(Mg_{0.4}, Fe_{0.6})_2SiO_4(sp) + 3aO_2$$
$$\rightarrow 2aFe_2O_3(hmt) + 2(Mg_{0.4}, Fe_{0.6-a})_2SiO_4(sp)$$

where a, ranging between 0 and 0.6, is the fraction of iron loss during oxidation.

Similar studies were carried out for Fe_2SiO_4, $(Fe_{0.2}, Mg_{0.8})_2SiO_4$, and Mg_2SiO_4 spinels at temperatures of up to 1100° C. The X-ray diffraction data obtained for Fe_2SiO_4-spinel quenched from various high temperatures are shown schematically in Figure 10. It shows that for those quenched from 500 and 600° C,

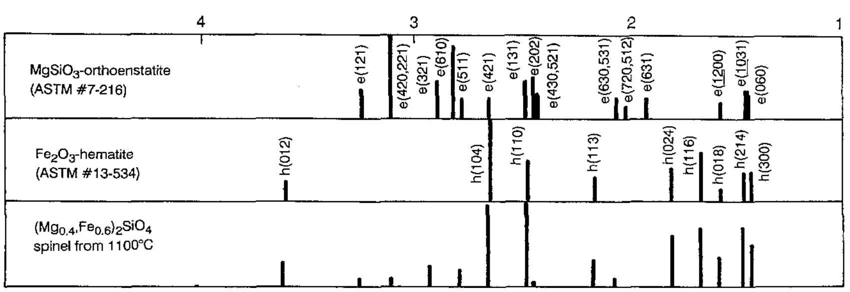

Fig. 9. Schematic X-ray diffraction diagrams showing that the end products (labelled as X) obtained by quenching the $(Mg_{0.4}, Fe_{0.6})_2SiO_4$-sp from 1000° C can be interpreted on the basis of hematite and enstatite phases shown on the top

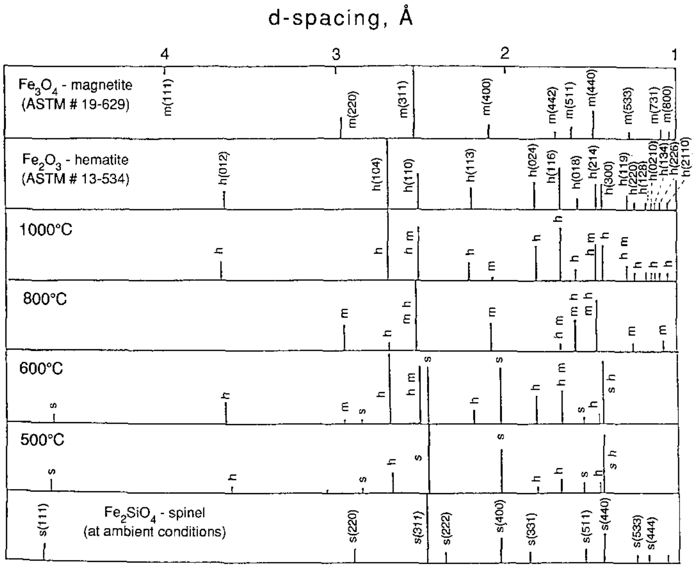

Fig. 10. Schematic X-ray diffraction diagrams obtained at ambient conditions for quenched samples of Fe_2SiO_4-sp from various high temperatures. Patterns of hematite and magnetite placed on top of this figure are for comparisions. Lines labelled with s, h, and m represent spinel, hematite, and magnetite, respectively

Table 5. X-ray diffraction data of Fe_2SiO_4-spinel quenched from 600° C (in air)

I/I_0	d(obs.)	Phases identified			
		Fe_2O_3*		Fe_2SiO_4(sp)**	
		(hkl)	d(cal.)	(hkl)	d(cal.)
15	4.702			(111)	4.718
30	3.685	(012)	3.689		
5	2.882			(220)	2.889
100	2.698	(104)	2.703		
95	2.518	(110)	2.524		
95	2.470			(311)	2.464
25	2.202	(113)	2.211		
90	2.048			(400)	2.043
40	1.836	(024)	1.845		
50	1.693	(116)	1.697		
10	1.573			(511)	1.572
15	1.483	(214)	1.489		
50	1.446	(300)	1.457		

* Calculated on the basis of $a = 5.029$ (5) Å and $c = 13.744$ (7) Å
** Calculated on the basis of $a = 8.172$ (20) Å

the product consists of only two phases: spinel and hematite (see Table 5 for the run at 600° C); for those from 800° C, the spinel phase is completely replaced by the magnetite and hematite phases (magnetite being more abundant, see Table 6); and for those samples quenched from temperatures above 900° C, it is almost a pure hematite phase (see Table 7 for the run at 1000° C). Lattice parameters for each of the phases present for each quenched sample (Table 8) show that the values for the hematite and magnetite quenched from different temperature conditions are in fairly good agreement with published data. However, the values obtained for spinels at 500 and 600° C are 8.181 Å and 8.172 Å, respectively, which are much smaller than that of the pure Fe_2SiO_4-spinel ($a = 8.247$ Å). These results indicate the spinel phase, coexisting with the hematite phase at temperatures below 800° C, is most likely to be deficient in iron due to the iron loss during oxidation. The oxidation reaction for Fe_2SiO_4-spinel is therefore summarized as:

Table 6. X-ray diffraction data of Fe_2SiO_4-spinel quenched from 800° C

I/Io	d(obs.)	Fe_3O_4		Fe_2O_3	
		(hkl)	d(cal.)*	(hkl)	d(cal.)**
10	4.855	(111)	4.852		
30	2.974	(220)	2.971		
10	2.697			(104)	2.709
100	2.536	(311)	2.534	(110)	2.532
30	2.098	(400)	2.101		
10	1.706	(422)	1.715	(116)	1.701
40	1.616	(511)	1.617	(018)	1.604
60	1.490	(440)	1.486	(214)	1.493
10	1.285	(533)	1.282		
15	1.094	(731)	1.094		

* Calculated on the basis of $a = 8.404(2)$ Å
** Calculated on the basis of $a = 5.0634(8)$ Å, and $c = 13.783(20)$ Å

Table 7. X-ray diffraction data of Fe_2SiO_4-spinel quenched from 1000° C

I/I_0	d(obs.)	Phases identified			
		Fe_2O_3*		Fe_3O_4**	
		(hkl)	d(cal.)	(hkl)	d(cal.)
30	3.690	(012)	3.689		
100	2.699	(104)	2.703		
100	2.520	(110)	2.524	(311)	2.513
25	2.216	(113)	2.211		
5	2.087			(400)	2.084
50	1.844	(024)	1.845		
75	1.698	(116)	1.697	(422)	1.702
15	1.601	(018)	1.600	(511)	1.604
50	1.492	(214)	1.489		
50	1.454	(300)	1.457		
20	1.309	(119)	1.307		
10	1.265	(220)	1.262		
10	1.165	(0210)	1.143		
10	1.144	(134)	1.164		
10	1.104	(226)	1.106		
10	1.058	(2110)	1.057		
10	1.046	(1112)	1.044		

* Calculated on the basis of $a = 5.0470$ (2) Å and $c = 13.763$ (5) Å
** Calculated on the basis of $a = 8.336$ (2) Å

(i) At $T < 600°$ C

$$2Fe_2SiO_4(sp) + 3/2\,O_2 \rightarrow a\,Fe_2O_3(hmt) + 2\,Fe_{2-a}SiO_4(sp)$$

(ii) At $T = 800$–$900°$ C

$$(2a + 3b)\,Fe_2SiO_4(sp) + (a + b)\,O_2 \rightarrow 2a\,Fe_2O_3(hmt) + 2b\,Fe_3O_4(mgt) + (2a + 3b)\,SiO_2(x)$$

Table 8. Zero-pressure lattice parameters of spinel, hematite and magnetite phases obtained by quenching Fe_2SiO_4-spinel from elevated temperatures

Temperature (°C)	Spinel ($a=8.347$ Å)^a	Hematite ($a=5.034$ Å,	$c=13.796$ Å)^b	Magnetite ($a=8.347$ Å)^c
	a, Å	a, Å	c, Å	a, Å
500	8.181	5.027 (7)	13.731 (9)	–
600	8.172	5.029 (5)	13.744 (7)	–
800	–	5.063 (8)	13.783 (20)	8.404
900	–	5.055 (3)	13.791 (11)	–
1000	–	5.047 (2)	13.763 (5)	–
1100	–	5.034 (1)	13.807 (5)	–

[a] This study, [b] ASTM 19-629, [c] ASTM 13-534

Table 9. X-ray diffraction data of $(Mg_{0.8}, Fe_{0.2})_2SiO_4$-spinel quenched from 1000° C

I/Io	d(obs.)	Phases identified					
		Fe_2O_3		Fe_3O_4		Mg_2SiO_4(ol)	
		(hkl)	d(cal.)*	(hkl)	d(cal.)**	(hkl)	d(cal.)***
40	3.905					(021)	3.876
20	3.716					(101)	3.727
30	2.981			(220)	2.973	(002)	2.982
20	2.875					(012)	2.862
20	2.761					(130)	2.770
40	2.692	(104)	2.702				
100	2.520	(110)	2.514	(311)	2.536		
						(131)	2.512
90	2.456					(112)	2.455
40	2.263					(122)	2.266
						(140)	2.250
5	2.100			(400)	2.103		
20	1.835	(024)	1.840				
40	1.746					(222)	1.750
5	1.699	(116)	1.695				
40	1.611	(018)	1.061	(511)	1.619	(133)	1.611
80	1.485	(214)	1.485	(440)	1.487	(062)	1.477
5	1.394					(170)	1.394
						(233)	1.393
5	1.354					(322)	1.353
5	1.313	(119)	1.307			(134)	1.313

* Calculated on the basis of a hexagonal unit cell with $a=5.030(10)$ Å, and $c=13.781(13)$ Å

** Calculated on the basis of a cubic unit cell with $a=8.410(20)$ Å

*** Calculated on the basis of an orthorhombic unit cell with $a=4.773(21)$ Å, $b=10.203(40)$ Å, and $c=5.964(35)$ Å

(iii) At $T>1000°$ C

$$2Fe_2SiO_4(sp)+O_2 \rightarrow 2Fe_2O_3(hmt)+2SiO_2(x)$$

As none of the X-ray diffraction lines from the Fe_2SiO_4 spinel quenched from various high temperatures can positively be assigned to any SiO_2 polymorph, it appears that the SiO_2 phase resulting from the reactions of (ii) and (iii) above is in the amorphous state.

In the case of $(Mg_{0.8}, Fe_{0.2})_2SiO_4$-spinel, X-ray diffraction data show that at 1000° C, except for one line at $d=3.716$ Å, all the data can be reasonably explained by a mixture of hematite, magnetite, and forsterite (see Table 9). The zero-pressure lattice parameters calculated for each of the phases are $a=5.030(10)$ Å and $c=13.781(13)$ Å for the hematite phase; $a=8.410(20)$ Å for the magnetite phase; and $a=4.773(21)$ Å, $b=10.203(40)$ Å and $c=5.964(35)$ Å for the forsterite phase. These values are in good agreement with the published values (i.e., for hematite: $a=5.034$ Å, $c=13.752$ Å (ASTM # 19-629); for magnetite: $a=8.397$ Å (ASTM # 13-534); and for forsterite: $a=4.758$ Å, $b=10.207$ Å and $c=5.988$ Å (ASTM # 7-74)) indicating that all the iron in the spinel is probably oxidized into Fe_2O_3 plus Fe_3O_4 and that the olivine phase has the Mg_2SiO_4 composition. Assuming that the mole fraction of Fe_2O_3 and Fe_3O_4 are a and b, respectively, the oxidation reaction in $(Mg_{0.8}, Fe_{0.2})_2SiO_4$-spinel at 1000° C can be represented as follows:

$$\begin{aligned}&(2a+3b)(Fe_{0.2}, Mg_{0.8})_2SiO_4+0.2(a+b)O_2\\&\rightarrow 0.4a\,Fe_2O_3+0.4b\,Fe_3O_4\\&\quad+0.8(2a+3b)\,Mg_2SiO_4+0.2(2a+3b)\,SiO_2\end{aligned}$$

In the case of pure Mg_2SiO_4-spinel, it converts completely back to olivine phase at 1000° C.

In summary, the present study demonstrates that by heating $(Mg,Fe)_2SiO_4$-spinels in vacuum, all the spinels transform back into their corresponding olivine phase via the nucleation and growth mechanism. However, on heating the $(Mg,Fe)_2SiO_4$-spinels in air, except for the pure end member of Mg_2SiO_4, all the iron-bearing $(Mg,Fe)_2SiO_4$ spinels are oxidized. The end products depend not only on the Fe/Mg ratio in the spinel phase but also on the quenched temperature. The oxidation of Fe-rich spinels starts at temperatures as low as 300–400° C. Thus caution is required in interpreting results from any measurements in air at higher temperatures. In view of this, the anomalously high thermal expansivity observed for the Fe_2SiO_4-spinel (Takeuchi et. al. 1984; Yamanaka 1986) and the iron-rich $(Mg,Fe)_2SiO_4$ spinels (Ming et al. 1987, 1988) are probably the result of such an oxidation effect.

Acknowledgment. The authors thank the staff of the Stanford Synchrotron Radiation Laboratory for providing the facilities for this research, J.-A. Xu, R. Secco, and L.-J. Wang for helpful discussions. This research was supported by the Earth Science Division, National Science Foundation (NSF Grant EAR87-08482). School of Ocean and Earth Science and Technology Contribution number No. 2373.

References

Akimoto S, Fugisawa H (1968) Olivine-spinel solid solution equilibria in the system Mg_2SiO_4-Fe_2SiO_4. J Geophys Res 73:1467–1479

Akimoto S, Akaogi M, Kamada K, Nishizawa O (1976) Mineralogic distribution of iron in the upper half of the transition zone in the earth's mantle. In: Sutton GH, Manghnani MH, Moberly R (eds) The Geophysics of the Pacific Ocean Basin and Its Margin, Geophys. Monogr. Ser., 19. AGU, Washington, D.C., pp 399–405

Bina GR, Wood BJ (1987) Olivine-spinel transitions: experimental and thermodynamic constraints and implications for the nature of the 400-km seismic discontinuity. J Geophys Res 92:4853–4866

Boland JN, Liu L (1983) Olivine to spinel transformation in Mg_2SiO_4 via faulted structures. Nature 303:233–235

Brar NS, Schloessin HH (1981) The kinetic of the GeO_2 (α-quartz)-→(rutile) transformation under high pressure. High pressure and High Pressure 13:313–320

Cahn JW (1956) The kinetics of grain boundary nucleated reactions. Acta Metall 4:449–459

Christian JW (1975) The Theory of Transformations in Metals and Alloys, Part I. Pergamon, New York, pp 586

Furnish MD, Bassett WA (1983) Investigation of the mechanism of the olivine-spinel transition in fayalite by synchrotron radiation. J Geophys Res 88(B12):10333–10341

Hamaya H, Akimoto S (1982) Experimental investigation of olivine-spinel transformation: growth of single crystal spinel from single crystal olivine in Ni_2SiO_4. In: Akimoto S, Manghnani MH (eds) High Pressure Research in Geophysics. Center for Acad Publ Japan, Tokyo, pp 362–373

Hazen RM (1977) Effects of temperature and pressure on the crystal structure of ferromagnesia olivine. Am Mineral 62:286–295

Jahanbagloo IC (1969) X-ray diffraction study of olivine solid solution series. Am Mineral 54:246–251

Jeanloz R, Thompson AB (1983) Phase transitions and mantle discontinuities. Rev Geophys 21:51–74

Katsura T, Ito E (1989) The system Mg_2SiO_4-Fe_2SiO_4 at high pressures and temperatures: precise determination of stabilities of olivine, modified spinel and spinel. J Geophys Res 94(10):15663–15670

Kawada K (1977) The system $Mg_2SiO_4-Fe_2SiO_4$ at high pressures and temperatures and the Earth's interior. Ph.D. Thesis, University of Tokyo, Tokyo

Knittle E, Jeanloz R (1987) The activation energy of the back transformation of silicate perovskite to enstatite. In: Manghnani MH, Syono Y (eds) High-Pressure Research in Mineral Physics. Terra Sci. Pub. Co., Tokyo/American Geophys Union, Washington, D.C., pp 69–74

Lacam A, Madon M, Poirier JP (1980) Olivine glass and spinel formed in a heated, diamond-anvil high pressure cell. Nature 2889:155–157

Manghnani MH, Ming LC, Nakagiri N (1987) Investigation of α-Fe→ε-Fe phase transition and the equation of state of the ε-Fe phase by synchrotron radiation. In: Manghnani MH, Syono Y (eds) High Pressure Research in Mineral Physics. Terrapub/AGU, pp 155–164

Ming LC, Manghnani MH (1988) High pressure and high temperature X-ray diffraction studies using the diamond anvil cell with synchrotron radiation. In: Barto-Kyriakidis A (ed) Synchrotron Radiation Applications in Mineralogy and Petrology, 33–48. Theophrastus Pub., Athens, pp 33–48

Ming LC, Manghnani MH, Qadri SQ, Skelton EF, Jamieson JC, Balogh J (1983) Gold as a reliable internal pressure calibrant at high temperatures. J Appl Phys 54(18):4390–4397

Ming LC, Manghnani MH, Balogh J (1987) Resistive heating in the diamond anvil cell under vacuum conditions. In: Manghnani MH, Syono Y (eds) High-Pressure Research in Mineral Physics (The Akimoto Volume). Terra Sci. Pub. Co., Tokyo/American Geophys Union, Washington, D.C., pp 69–74

Poirier JP (1982) The kinetics of martensitic olivine γ-spinel transition and its dependence on materials and experimental parameters. In: Akimoto S, Manghnani MH (eds) High-Pressure Research on Geophysics. Center for Acad Publ Japan/Tokyo, pp 361–372

Ringwood AE (1975) Composition and Petrology of the Earth's Mantle. McGraw-Hill, New York

Ringwood AE, Major A (1970) The system $Mg_2SiO_4-Fe_2SiO_4$ at high pressure and temperatures. Phys Earth Planet Inter 3:89–108

Smyth JR (1975) High temperature crystal chemistry of fayalite. Am Mineral 60:1092–1097

Suito K (1972) Phase transformations of pure Mg_2SiO_4 in to a spinel structure under high pressures and temperatures. J Phys Earth 20:225–243

Suito K (1977) Phase relations of pure Mg_2SiO_4 up to 200 kbar. In: Manghnani MH, Akimoto S (eds) High-Pressure Research: Applications to Geophysics. Academic Press, New York, pp 255–266

Sung CM, Burns RG (1976a) Kinetics of the olivine-spinel transition: implications to deep-focus earthquake genesis. Earth Planet Sci Lett 32:165–170

Sung CM, Burns RG (1976b) Kinetics of high-pressure phase transformations: implications to the evolution of olivine-spinel transition in the downgoing lithosphere and its consequences on the dynamics of the mantle. Tectonophysics 31:1–32

Takeuchi Y, Yamanaka T, Haga N, Hirano M (1984) High temperature crystallography of olivines and spinels. In: Sunagawa I (ed) Materials Science of the Earth's Interior. TERRAPUB, Tokyo, pp 191–231

Weidner DJ (1985) A mineral physics test of a pyrolite mantle. Geophys Res Lett 12:417–420

Weidner DJ, Ito E (1987) Mineral physics constraints on uniform mantle composition. In: Manghnani MH, Syono Y (eds) High-Pressure Research in Mineral Physics (The Akimoto Volume). Terra Sci. Pub. Co., Tokyo/American Geophys Union, Washington, D.C., pp 439–446

Yamanaka T (1986) Crystal structures of Ni_2SiO_4 and Fe_2SiO_4 as a function of temperature and heating duration. Phys Chem Minerals 13:227–232

Zeto RJ, Roy R (1969) Kinetics of the GeO_2(quartz)$-GeO_2$(rutile) transformation at pressure at pressures to 30 kbar. In: Mitchell JW et al. (eds) Reactivity of Solids, Proceedings of the 6th International Symposium on Reactivity of Solids. Wiley, New York, pp 803–815